Comparative Analysis of Different Single-Diode PV Modeling Methods

Samkeliso Shongwe, *Member, IEEE*, and Moin Hanif, *Member, IEEE*

Abstract—Modeling of photovoltaic (PV) systems is essential for the designers of solar generation plants to do a yield analysis that accurately predicts the expected power output under changing environmental conditions. This paper presents a comparative analysis of PV module modeling methods based on the single-diode model with series and shunt resistances. Parameter estimation techniques within a modeling method are used to estimate the five unknown parameters in the single diode model. Two sets of estimated parameters were used to plot the *I–V* characteristics of two PV modules, i.e., SQ80 and KC200GT, for the different sets of modeling equations, which are classified into models 1 to 5 in this study. Each model is based on the different combinations of diode saturation current and photogenerated current plotted under varying irradiance and temperature. Modeling was done using MATLAB/Simulink software, and the results from each model were first verified for correctness against the results produced by their respective authors. Then, a comparison was made among the different models (models 1 to 5) with respect to experimentally measured and datasheet *I–V* curves. The resultant plots were used to draw conclusions on which combination of parameter estimation technique and modeling method best emulates the manufacturer specified characteristics.

Index Terms—Modeling, one-diode model, parameter estimation, photovoltaic (PV) model, renewable energy.

I. INTRODUCTION

SOLAR power stations rely on the energy from the sun, which is readily available to produce electricity using photovoltaic (PV) panels [1]. It is one of the few abundantly available options as the world turns to renewable energy sources as a means to produce clean energy. In [2], it is revealed that by 2030, renewable energy could contribute 42% of the South African power demand because it is becoming increasingly competitive with ESKOM tariffs, which use mainly fossil fuels for electricity generation. It is also mentioned that there has been a reduction in solar tariffs over three successive bidding rounds of renewable energy-independent power producer procurement program from R3/kWh to R1/kWh, showing the great potential of growth in solar power generation.

PV generation plants consist of a number of components used for power conditioning, which are connected to the PV panels. The main aim of an accurate mathematical model of a PV panel, module, or cell is to optimize the design and dimensioning of PV power plants to maximize their power generation capability [3], as well as to be able to accurately define specifications for the power conditioning equipment. Modeling involves mathematically expressing the behavior of PV module current and power with respect to voltage under varying temperature and irradiance. Batzelis *et al.* [4] presented another characteristic, which expresses voltage with respect to current by using the lambert W function. This required that some or a part of the expressions be neglected to simplify the computation, and this affects the accuracy of the end result. It also introduces complexity as it requires the evaluation of the Lambert W function.

As per the literature, single-diode model, which has different variants, and the double-diode model [5], [6] have been widely used. Bal *et al.* [7] and Suthar *et al.* [8] compared the different variations of the single-diode model with the two-diode model for a PV panel. In all cases, the single-diode model, which consists of a series resistor and a parallel resistor connected across a diode and a current source was selected as the best, considering accuracy as well as complexity, and thus will be used in this study.

Work has been done to model PV characteristics using different techniques. Suskis *et al.* [1], [9]–[14] have developed models by using experimental data. An experiment is set up using a specific module to measure the output voltage and current under different conditions to produce the characteristic plot, which is then used to evaluate all parameters required for the model. Andrei *et al.* [15] used a curve fitting technique to find the parameters for modeling. Even though a more practical result is obtained, this kind of approach, however, has the limitation of producing a model which is specific to that module, whereas a more general modeling technique is required which can be applicable to any module with the given datasheet parameters.

A better approach is to formulate equations or expressions for all the unknown parameters based on different modes of operation of the PV modules namely, open-circuit operation, short-circuit operation, and maximum power point operation, [16]–[20]. However, this poses a challenge since these equations are nonlinear and transcendental in nature; therefore, it is difficult to find explicit solutions for them [21].

A number of iteration methods, termed numerical methods [22] have been used to find solutions to these equations. Chatterjee *et al.* [16] uses Gaussian Iteration method, while Sera *et al.* [23] uses Newton–Raphson method to solve the system of equations and Jun and Kay-Soon [19], [24] use particle swarm optimization.

Another approach, classified as an analytical method in [22], estimates one of the parameters to simplify the computation, but this may pose inaccuracies if the estimation is not accurate. Villalva *et al.* [25] assumed a value of ideality factor and

This article has been accepted for inclusion in a future issue of this journal. Content is final as presented, with the exception of pagination.

2   IEEE JOURNAL OF PHOTOVOLTAICS

evaluated the other parameters, and Chatterjee *et al.* [16] and Mahmoud *et al.* [17] make the assumption that $I_{ph} = I_{sc}$ leaving only four parameters unknown. In addition, Mahmoud *et al.* [17] defined a way to estimate the shunt resistance, which is then used to evaluate the other four parameters from the equations. This, however, requires that the estimation be as accurate as possible; otherwise, ridiculous values can be obtained which are far from the expected ones.

Another approach to find the parameters is to use the equations but instead of estimation, one of the parameters is adjusted such that the corresponding values of current obtained matches a specific known condition, such as the maximum power point where the current and voltage are always known from datasheets. Moballegh and Jiang [13], [25]–[27] choose values of series resistance starting from zero and incrementing the resistance until a specified and acceptable margin of error exists between the calculated value and the maximum power point values. Rahman *et al.* [18], on the other hand, use the same technique but with a variation of the ideality factor based on the fact that its value ranges from 1 to 2.

All of the above described work evaluates the parameters at one known condition, i.e., the standard test condition (STC): defined as a temperature of 25 °C and irradiance equal to 1000 W/m^2 [20], at which the datasheet parameters are generally specified. They also assume that the values of resistances at conditions other than STC remain unchanged such that the only parameters which are calculated are the photocurrent and the saturation current. These parameters are dependent on the temperature and irradiance [28], and as such, there are a few different ways in which they are represented.

After a thorough review on the literature based on the PV system modeling, it was established that there are five unique combinations of photogenerated currents and reverse saturation currents which have been used and these combinations are classified as *model 1* used in [16] and [23], *model 2* in [19], [25], [27], and [29], *model 3* used by Mahmoud *et al.* [17] and [21], *model 4* in [5], [6], [8], [30], and [31], and *model 5* used by Siddique *et al.* [20] in this study.

This paper presents a comparative analysis of the five models, classified as above. The first step involves using the two different parameter estimation methods as follows:

1) Gaussian iteration [16];
2) adjustment of series resistance to match the maximum power point [25].

Parameters at STC for the SQ80 [32] and KC200GT [34] modules are estimated using the above two methods. These parameters are then used to evaluate and plot the *I–V* characteristic of the two PV modules at different values of temperature and irradiance using the five models classified in this study. A comparison is made with the characteristic plots obtained from experimental measurements on the SQ80 module and plots contained in the datasheet of the KC200GT module [34]. All computations done in this paper are done using MATLAB/Simulink. Based on the comparison, the model which produces a graph that closely resembles the plot from measured values and the one on the datasheet can be selected as the most accurate one.
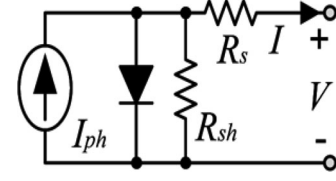

Fig. 1. Equivalent circuit for single-diode model.

Section II of this paper describes the two different parameter estimation methods used in this analysis and goes on to describe the five different models to be compared. In Section III, the results obtained from the simulations and measurements are presented, as well as the extracts from the datasheet. These results are briefly discussed in this section and then a conclusion is outlined in Section IV.

II. Modeling of Photovoltaic Array

The main task in modeling involves producing a graph depicting the behavior of the PV array output current and power, with respect to the voltage under different environmental conditions (temperature and irradiance). Modeling requires two steps; the first step is parameter estimation, and the second is to use these estimated parameters within the modeling equations that produce the graph depicting the behavior of the modules under varying temperature and irradiance.

Fig. 1 [3] shows the single-diode equivalent circuit of a PV cell and the relationship between the current and voltage at the terminals of the PV cell is represented by

$$I = I_{ph} - I_0 \left[\exp \left(\frac{V + IR_s}{N_s V_t} \right) - 1 \right] - \frac{V + IR_s}{R_{sh}} \quad (1)$$

where I is the module current; V is the module voltage; I_{ph} is the photogenerated current; I_0 is the diode reverse saturation current; R_s is the series resistance; R_{sh} is the shunt resistance; N_s is the number of series connected cells in the module; V_t is the junction thermal voltage and can be expressed as $V_t = \frac{kAT}{q}$, where k is the Boltzmann's constant equal to 1.38×10^{-23} J/K; q is the electron charge equal to 1.602×10^{-19} C; and A is the diode ideality constant. A relationship between the current flowing and the voltage across the PV array is described in (1). It is, therefore, essential that the values of the other parameters in (1) are found to complete the relationship and hence the model. Five unknown parameters exist in (1), which are: I_{ph}, I_0, R_s, R_{sh}, and A. N_s is always readily available in PV module datasheets.

A. Parameter Estimation

Two estimation methods 1) and 2) listed above are considered in this paper. Method 1) uses iterative solution of equations as recommended by Chatterjee *et al.* [16] and method 2) uses maximum power point matching [25]. The values obtained using these methods are valid under STC. Both parameter estimation methods consider three conditions of operation of a PV

This article has been accepted for inclusion in a future issue of this journal. Content is final as presented, with the exception of pagination.

SHONGWE AND HANIF: COMPARATIVE ANALYSIS OF DIFFERENT SINGLE-DIODE PV MODELING METHODS
3

module, i.e., open-circuit, short-circuit, and maximum power point operation.

1) *Open-circuit condition:* This is the condition where the output terminals of the PV module are not connected, and the voltage across the PV module terminals is at its highest and equal to open-circuit voltage V_{oc}. There is no current flowing at the output, and thus, $I = 0$.

2) *Short-circuit condition:* This is the condition where the output terminals of the PV module are connected together (shorted) such that the voltage across the PV panel $= 0$. The highest value of current will flow across the PV module at this point and is equal to the short-circuit current I_{sc}.

   In addition, under the same condition, the derivative of the current with respect to voltage $\frac{dI}{dV} = \frac{-1}{R_{\mathrm{sho}}}$ obtained from the slope of the I–V characteristic in the region closer to the short-circuit condition, where R_{sho} is the effective resistance under short-circuit conditions; in this paper, we will, however, assume that $R_{\mathrm{sho}} = R_{\mathrm{sh}}$.

3) *Maximum power point:* At maximum power point operation, the current flowing at the output of the PV module is equal to I_{mp} and the voltage across the PV module is equal to V_{mp}. In addition, the derivative of power with respect to voltage $\frac{dP_{mp}}{dV_{mp}} = 0$ at the maximum power point.

1) Estimation Method A: Method A considers the three conditions of operation of a PV module as described above to come up with five conditions resulting in five equations with the five unknown parameters, which are then solved by using an iteration method, i.e., Gaussian Iteration [16]

$$I_o = \frac{I_{\mathrm{sc}}R_{\mathrm{sh}} + I_{\mathrm{sc}}R_s - V_{\mathrm{oc}}}{R_{\mathrm{sh}}\exp\left(\frac{V_{\mathrm{oc}}}{N_s V_t}\right)} \tag{2}$$

$$I_{\mathrm{ph}} = I_o\left[\exp\left(\frac{V_{\mathrm{oc}}}{N_s V_t}\right) - 1\right] + \frac{V_{\mathrm{oc}}}{R_{\mathrm{sh}}} \tag{3}$$

$$V_t = \frac{V_{mp} + I_{mp}R_s - V_{\mathrm{oc}}}{N_s\ln\left(\frac{I_{\mathrm{sc}}R_{\mathrm{sh}}+I_{\mathrm{sc}}R_s-V_{\mathrm{oc}}-V_{mp}-I_{mp}R_s-I_{mp}R_s}{I_{\mathrm{sc}}R_{\mathrm{sh}}+I_{\mathrm{sc}}R_s-V_{\mathrm{oc}}}\right)} \tag{4}$$

[see also (5) and (6) at the bottom of the page]. Equations (2)–(6) are used to estimate the values. A program is developed in MATLAB to implement the Gaussian Iteration method using the equations above. The solutions obtained are given in Tables I and II.

2) Estimation Method B: Method B involves reducing the number of equations to four by estimating one of the parameters, while comparing the maximum power point as recommended

TABLE I
SQ80 STC PARAMETERS ESTIMATED USING METHOD A AND METHOD B

Parameter	Estimated value	
	Method A	Method B
R_s	0.3085 Ω	0.3763 Ω
R_{sh}	1.676 kΩ	1.005 kΩ
V_t	0.02739 V	0.0243 V
I_o	1.207×10^{-9}	6.967×10^{-11}
I_{ph}	4.85 A	4.8518 A
A	1.067	0.95

TABLE II
KC200GT STC PARAMETERS ESTIMATED USING METHOD A AND METHOD B

Parameter	Estimated value	
	Method A	Method B
R_s	0.2163 Ω	0.29 Ω
R_{sh}	993.0 Ω	160.3 Ω
V_t	0.0345 V	0.02739 V
I_o	1.772×10^{-7} A	2.179×10^{-9} A
I_{ph}	8.212 A	8.21 A
A	1.343	1.067

by Villalva *et al.* [25] and Islam *et al.* [27]. The same idea was used by Siddique *et al.* [20], where A is perturbed instead of R_s. The derived equations used in this method [25], [33] are as follows:

$$I_{\mathrm{ph,STC}} = \frac{R_s + R_{\mathrm{sh}}}{R_{\mathrm{sh}}}I_{\mathrm{sc}}. \tag{7}$$

At initial conditions $R_s = 0$, (7) reduces to

$$I_{\mathrm{ph,STC}} = I_{\mathrm{sc}} \tag{8}$$

$$A = \frac{K_v - \frac{V_{\mathrm{oc}}}{T_{\mathrm{STC}}}}{N_s V_T\left(\frac{K_I}{I_{\mathrm{ph,STC}}} - \frac{3}{T_{\mathrm{STC}}} - \frac{qE_g}{kT_{\mathrm{STC}}^2}\right)} \tag{9}$$

$$R_{\mathrm{sh(in)}} = \frac{V_{mp}}{I_{\mathrm{sc}} - I_{mp}} - \frac{V_{\mathrm{oc}} - V_{mp}}{I_{mp}} \tag{10}$$

$$I_o = \frac{I_{\mathrm{sc}}}{R_{\mathrm{sh}}\exp\left(\frac{V_{\mathrm{oc}}}{N_s V_t}\right)}. \tag{11}$$

In the above equations, $R_{\mathrm{sh(in)}}$ is the initial value of R_{sh}, shown as (12) at the bottom of the next page, and K_v and K_I are the temperature coefficients for voltage and current, respectively. A flowchart showing the steps followed in imple-

$$R_s = \frac{V_{\mathrm{oc}} - V_{mp} + N_s V_t\ln\left[\frac{N_s V_t R_{\mathrm{sh}}I_{mp}-N_s V_t V_{mp}+N_s V_t I_{mp}R_s}{(V_{mp}I_{\mathrm{sc}}R_{\mathrm{sh}}+V_{mp}I_{\mathrm{sc}}R_s-V_{mp}V_{\mathrm{oc}}+I_{mp}R_s V_{\mathrm{oc}}-I_{mp}R_s I_{\mathrm{sc}}R_s-I_{mp}R_s R_{\mathrm{sh}}I_{\mathrm{sc}})}\right]}{I_{mp}} \tag{5}$$

$$R_{\mathrm{sh}} = \frac{N_s V_t R_{\mathrm{sh}} + (R_s I_{\mathrm{sc}}R_{\mathrm{sh}} + R_s I_{\mathrm{sc}}R_s - R_s V_{\mathrm{oc}})\exp\left(\frac{I_{\mathrm{sc}}R_s-V_{\mathrm{oc}}}{N_s V_t}\right) + N_s V_t R_s}{(I_{\mathrm{sc}}R_{\mathrm{sh}} + I_{\mathrm{sc}}R_s - V_{\mathrm{oc}})\exp\left(\frac{I_{\mathrm{sc}}R_s-V_{\mathrm{oc}}}{N_s V_t}\right) + N_s V_t}. \tag{6}$$

This article has been accepted for inclusion in a future issue of this journal. Content is final as presented, with the exception of pagination.

4   IEEE JOURNAL OF PHOTOVOLTAICS
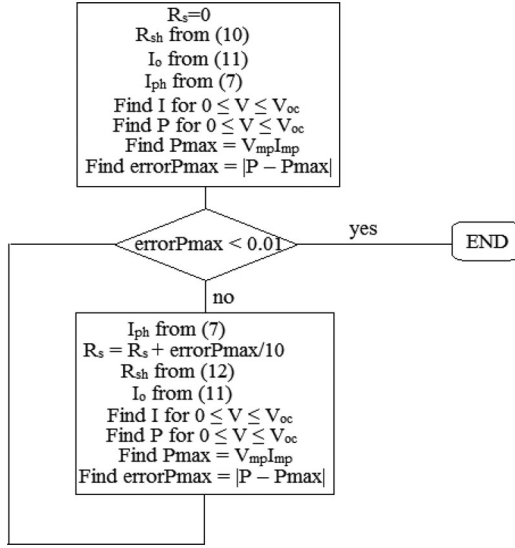

Fig. 2.   Algorithm for parameter estimation in method B.

menting this method is illustrated in Fig. 2 [25]. The computation of this algorithm is also done in MATLAB, and the solutions are given in Tables I and II.

B. Different Modeling Equations

The operation of PV arrays is normally under changing atmospheric conditions, which will be affected by the overall irradiance and temperature under which the PV array is operated. These conditions have an effect on the overall output of the PV array. It is, therefore, essential that they are considered during the modeling of the PV module. Most of the modeling work considers that the ideality factor, the series resistance, and the shunt resistance are constant with varying temperature; thus, they are assumed not to change with temperature [24].

The only parameters which are considered to change with temperature and irradiance are I_o and I_{ph}. A modeling technique is made up by a combination of equations to evaluate these two parameters as functions of temperature and irradiance. Five combinations of equations are used in the literature for all mathematical models that are classified as follows:

Model 1 [16], [23]: Consider the temperature dependence of I_{sc} and V_{oc} given as follows:

$$V_{\mathrm{oc}}\left(T\right) = V_{\mathrm{oc}} + K_v \Delta T \tag{13}$$

$$I_{\mathrm{sc}}\left(T\right) = I_{\mathrm{sc}} + K_I \Delta T. \tag{14}$$

Equations (2) and (3) can be rewritten as (15), shown at the bottom of the next page.

$$I_{\mathrm{ph}} = G\left[I_o\left\{\exp\left(\frac{(V_{\mathrm{oc}}+K_v\Delta T)}{N_s V_t}\right) - 1\right\} + \frac{V_{\mathrm{oc}} + K_v\Delta T}{R_{\mathrm{sh}}}\right] \tag{16}$$

where T is the temperature of the module; ΔT is the temperature difference $T - T_{\mathrm{STC}}$; T_{STC} is the temperature at STC, which is equal to 298 K; and G is the ratio of the irradiance with respect to STC value equal to 1 kW/m^2. All temperatures are measured in Kelvin.

Model 2 [19], [25], [27], [29]: If we consider (8) as well as assume that the resistance R_{sh} is very high so that the second term on the right of (3) becomes zero and on rearranging, we get

$$I_o = \frac{I_{\mathrm{sc}}}{\exp\left(\frac{(V_{\mathrm{oc}})}{N_s V_t}\right) - 1}. \tag{17}$$

Considering the temperature dependence of I_{sc} and V_{oc} given in (12) and (13), (17) can be rewritten as

$$I_o = \frac{I_{\mathrm{sc}} + K_I \Delta T}{\exp\left(\frac{(V_{\mathrm{oc}}+K_v\Delta T)}{N_s V_t}\right) - 1} \tag{18}$$

$$I_{\mathrm{ph}} = (I_{\mathrm{ph,STC}} + K_I \Delta T)G. \tag{19}$$

Model 3 [17], [21]: In this model, it is assumed that (8) applies, by making I_o the subject in (3)

$$I_{o,\mathrm{STC}} = \frac{I_{\mathrm{ph,STC}} - \frac{V_{\mathrm{oc}}}{R_{\mathrm{sh}}}}{\exp\left(\frac{V_{\mathrm{oc}}}{N_s V_t}\right) - 1}. \tag{20}$$

Considering that the resistance R_{sh} is very high such that (20) becomes

$$I_{o,\mathrm{STC}} = \frac{I_{\mathrm{ph,STC}}}{\exp\left(\frac{V_{\mathrm{oc}}}{N_s V_t}\right) - 1}. \tag{21}$$

Making V_{oc} the subject of the formula in (21) and considering that $V_t = \frac{kAT}{q}$, we get

$$V_{\mathrm{oc}} = \frac{N_s kTA}{q}\ln\left(\frac{I_{\mathrm{ph,STC}}}{I_{o,\mathrm{STC}}} + 1\right). \tag{22}$$

Using the fact that $V_{\mathrm{oc}}\left(G,T\right) - V_{\mathrm{oc}}\left(G,T_{\mathrm{STC}}\right) = -|K_V|\Delta T$ and that $I_{\mathrm{ph}} = (I_{\mathrm{sc}} + K_i\Delta T)G$

$$\frac{N_s kTA}{q}\left[T\ln\left(\frac{G(I_{\mathrm{sc}}+K_I\Delta T)}{I_o}+1\right) - T_{\mathrm{STC}}\ln\left(\frac{GI_{\mathrm{sc}}}{I_{o,\mathrm{STC}}}+1\right)\right]$$
$$= -|K_V|\Delta T \tag{23}$$

$$I_o = \frac{G(I_{\mathrm{sc}} + K_I\Delta T)\exp\left(\frac{q|K_v|\Delta T}{N_s kTA}\right)}{\left(\frac{GI_{\mathrm{sc}}}{I_{o,\mathrm{STC}}}+1\right)^{\frac{T_{\mathrm{STC}}}{T}} - \exp\left(\frac{q|K_v|\Delta T}{N_s kTA}\right)} \tag{24}$$

$$I_{\mathrm{ph}} = (I_{\mathrm{ph,STC}} + K_I\Delta T)G \tag{25}$$

$$R_{\mathrm{sh}} = \frac{V_{mp}\left(V_{mp} + I_{mp}R_s\right)}{V_{mp}I_{\mathrm{ph}} + V_{mp}I_o - P_{\max} - V_{mp}I_o\exp\left(\frac{q\left(V_{mp}+I_{mp}R_s\right)}{N_s kAT}\right)}. \tag{12}$$

This article has been accepted for inclusion in a future issue of this journal. Content is final as presented, with the exception of pagination.

SHONGWE AND HANIF: COMPARATIVE ANALYSIS OF DIFFERENT SINGLE-DIODE PV MODELING METHODS

5

TABLE III
DATASHEET PARAMETERS

Parameter	SQ80	KC200GT
N_s	36	54
I_{sc}	4.85 A	8.21 A
V_{oc}	21.8 V	32.9 V
V_{mp}	17.5 V	26.3 V
I_{mp}	4.58 A	7.61 A
K_I	0.0014 A/°C	0.00318 A/°C
K_V	−0.081 V/°C	−0.123 V/°C
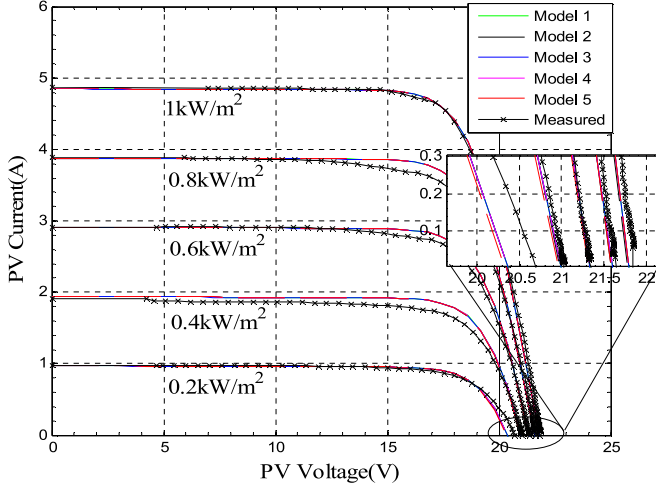
Fig. 3. *I–V* Characteristic for SQ80 module under varying irradiance for models 1, 2, 3, 4, and 5 and measured values, using parameter estimation method A.

Fig. 4. *I–V* Characteristic for SQ80 module under varying irradiance for models 1, 2, 3, 4, and 5 and measured values, using parameter estimation method B.

or

$$I_{ph} = (I_{sc} + K_I \Delta T)G. \tag{26}$$

Model 4 [5], [6], [8], [30], [31]: The saturation current is related to the bandgap and temperature by

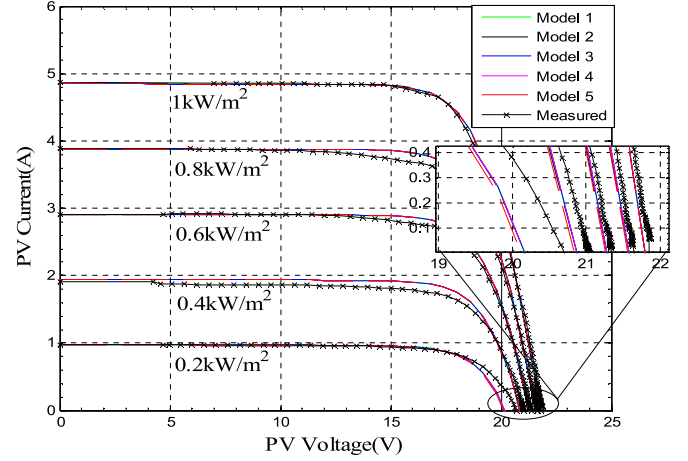$$I_o = D T^3 \exp\left(\frac{-qE_g}{AkT}\right) \tag{27}$$

where D is a constant dependent on the diffusion properties of the junction and E_g is the bandgap energy. Evaluating (27) at temperature T_{STC} and T results in

$$I_{o,STC} = D T_{STC}^3 \exp\left(\frac{-qE_g}{AkT_{STC}}\right) \tag{28}$$

$$I_o = D T^3 \exp\left(\frac{-qE_g}{AkT}\right). \tag{29}$$

Taking the ratio of (28) and (29) and rearranging results in

$$I_o = I_{o,STC} \left[\frac{T}{T_{STC}}\right]^3 \exp\left(\frac{qE_g}{Ak}\left(\frac{1}{T_{STC}} - \frac{1}{T}\right)\right) \tag{30}$$

$$I_{ph} = (I_{ph,STC} + K_i \Delta T)G. \tag{31}$$

Model 5 [20]: Using (1) under open-circuit conditions $I = 0$ and $V = V_{oc}$, and rearranging leads to

$$I_{ph,STC} = I_{o,STC}\left[\exp\left(\frac{V_{oc}}{N_s V_t}\right) - 1\right] + \frac{V_{oc}}{R_{sh}}. \tag{32}$$

In addition, using (1) under short-circuit conditions $I = I_{sc}$ and $V = 0$ leads to

$$I_{sc} = I_{ph,STC} - I_{o,STC}\left[\exp\left(\frac{I_{sc}R_s}{N_s V_t}\right) - 1\right] - \frac{I_{sc}R_s}{R_{sh}}. \tag{33}$$

Substituting for I_{ph} in (32) into (33) and rearranging leads to

$$I_{o,STC} = \frac{\left(1 + \frac{R_s}{R_p}\right)I_{sc} - \frac{V_{oc}}{R_p}}{\exp\left(\frac{V_{oc}}{V_t}\right) - \exp\left(\frac{I_{sc}R_s}{V_t}\right)}. \tag{34}$$

Considering temperature dependence of I_{sc} and V_{oc}, a new equation relating $V_{oc}(T)$ to the STC value is derived [20]

$$V_{oc}(T) = V_{oc} + K_v \Delta T + V_t \ln(G). \tag{35}$$

It is considered that there is dependence of V_{oc} on the irradiance; hence, the inclusion of the logarithmic factor in the equation. Substituting (13) for I_{sc} and (35) for V_{oc} into (34) results in

$$I_o = \frac{\left(1 + \frac{R_s}{R_p}\right)(I_{sc} + K_I \Delta T) - \frac{V_{oc} + K_v \Delta T + V_t \ln(G)}{R_p}}{\exp\left(\frac{V_{oc} + K_v \Delta T + \ln(G)}{V_t}\right) - \exp\left(\frac{(I_{sc} + K_I \Delta T)R_s}{V_t}\right)} \tag{36}$$

$$I_{ph} = (I_{ph,STC} + K_i \Delta T)G. \tag{37}$$

$$I_o = I_{sc,STC} + K_I(T - 298) - \frac{(V_{oc,STC} + K_V(T - 298)) - (I_{sc,STC} + K_I(T - 298))R_s}{R_{sh}\exp\left(\frac{(V_{oc,STC} + K_V(T - 298))}{N_s V_t}\right)} \tag{15}$$

This article has been accepted for inclusion in a future issue of this journal. Content is final as presented, with the exception of pagination.

6

IEEE JOURNAL OF PHOTOVOLTAICS

TABLE IV
SUMMARY OF GRAPHS UNDER VARYING IRRADIANCE

IRRADIANCE	Method A		Method B	
1 kW/m^2	Voc	I at $V = 20$	Voc	I at $V = 20$
Model 1	21.79534	2.77148	21.79381	2.88524
Model 2	21.79181	2.76704	21.79139	2.88223
Model 3	21.79181	2.76704	21.79363	2.884683
Model 4	21.79534	2.77148	21.79363	2.884683
Model 5	21.79534	2.77148	21.79363	2.884683
Measured	21.88	2.75	21.88	2.75
IRRADIANCE	Method A		Method B	
0.8 kW/m^2	Voc	I at $V = 20$	Voc	I at $V = 20$
Model 1	21.60401	2.22667	21.58055	2.258927
Model 2	21.60058	2.22277	21.57823	2.256272
Model 3	21.60369	2.22581	21.58038	2.258451
Model 4	21.60401	2.22667	21.58038	2.258451
Model 5	21.59883	2.22077	21.57462	2.251863
Measured	21.65	2.16	21.65	2.16
IRRADIANCE	Method A		Method B	
0.6 kW/m^2	Voc	I at $V = 20$	Voc	I at $V = 20$
Model 1	21.37035	1.62474	21.3248	1.589599
Model 2	21.36709	1.62142	21.32263	1.587297
Model 3	21.37006	1.62404	21.32464	1.589218
Model 4	21.37035	1.62474	21.32464	1.589218
Model 5	21.35909	1.61321	21.31234	1.576116
Measured	21.35	1.60	21.35	1.60
IRRADIANCE	Method A		Method B	
0.4 kW/m^2	Voc	I at $V = 20$	Voc	I at $V = 20$
Model 1	21.0772	0.96393	21.01241	0.877957
Model 2	21.07423	0.96118	21.01048	0.875997
Model 3	21.07695	0.96342	21.01229	0.877687
Model 4	21.0772	0.96393	21.01229	0.877687
Model 5	21.05879	0.94678	20.99259	0.857611
Measured	21.03	0.95	21.03	0.95
IRRADIANCE	Method A		Method B	
0.2 kW/m^2	Voc	I at $V = 20$	Voc	I at $V = 20$
Model 1	20.69795	0.24517	20.62332	0.125877
Model 2	20.69546	0.24298	20.62173	0.124239
Model 3	20.69779	0.24489	20.62324	0.125735
Model 4	20.69795	0.24517	20.62324	0.125735
Model 5	20.67083	0.22097	20.59488	0.096074
Measured	20.71	0.25	20.71	0.25

Fig. 5. *I–V* Characteristic for KC200GT module under varying irradiance for models 1, 2, 3, 4, and 5 using parameter estimation method A.

The five models described above have first been verified against the results produced by their respective authors and have been found to match, which renders the accuracy of further using them to be valid.

III. RESULTS AND DISCUSSIONS

The Shell SQ80 [32] and KC200GT [34] modules, whose datasheet parameters specified under STC are given in Table III, were used to evaluate and test the different modeling methods discussed in the previous section. The parameters estimated using the two parameter estimation methods for the two PV modules are already shown in Tables I and II.

Experimental measurements were taken using the SQ80 module connected to the PVPM curve plotter. The setup is shown in Fig. 8. The PVPM2540-C curve plotter was configured to take data samples every 30 s for one full day. At each sampling instance, it measured a full set of readings for current, voltage, temperature, and irradiance and then transferred the data to the connected PC via a serial interface. The experimental readings were extracte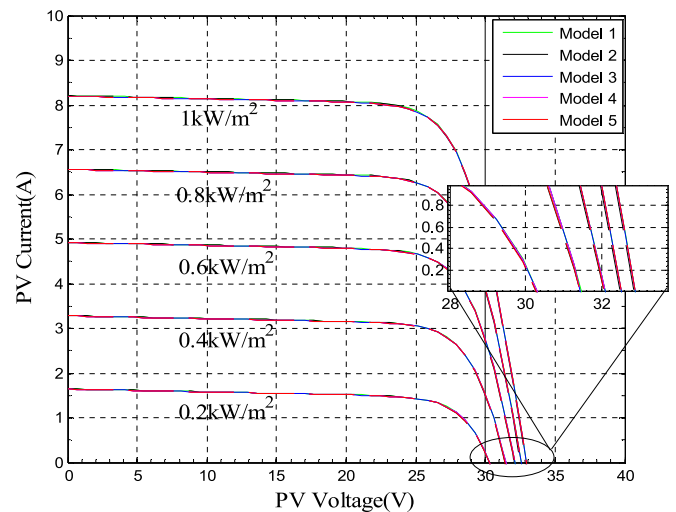d and included in the simulation plots for comparison. It should be noted that the curve plotter datasheet indicates an uncertainty of peak power measurement and a/d converter accuracy as $+/-5\%$ and $+/-0.25\%$, respectively. The graphs shown in Figs. 3 and 4 depict the results under varying irradiance for all five models using method A and method B, respectively, as well as includes plots using experimentally measured data for the SQ80 module.

Figs. 3 and 4 show that the open-circuit voltage response to changes in irradiance is the same for all the modeling methods described in this paper. In (36), i.e., saturation current in model 5, a factor is introduced which is meant to cater for dependence of open-circuit voltage on the irradiance. In inclusion of this factor, Siddique *et al.* [20] explained that there is a logarithmic dependence between the voltage and the irradiance, but Figs. 3 and 4 clearly show that the dependence of open-circuit voltage on irradiance is minimal.

The similarity of the short-circuit current response from all models was expected since in all the recommended modeling methods, the equation used for calculating I_{ph} is the same except for model 1. In comparison to the plot using experimental values, it can be seen that the response in terms of the short-circuit values is the same for both plots again owing to the comparable results found for I_{ph} using the two methods. However, considering the response as far as the open-circuit voltage is concerned, a small difference can be seen from the two plots and the graph, which shows results closer to the experimental results is the one in Fig. 3, using method A to estimate parameters.

Table IV gives a clear summary of the variation of the open-circuit voltage value obtained from the two methods using the SQ80 module. The different methods produced different values of series resistance, and from the plots, the effect of correctly estimating the series resistance can be seen. It can also be noted that even at low irradiance, the accuracy is maintained.

Figs. 5 and 6 show graphs plotted using KC200GT parameters using the two methods under varying irradiance. Fig. 7 is an extract from the KC200GT module datasheet. The same can be observed from the graphs in Figs. 5 and 6 when compared with the datasheet plot in Fig. 7.
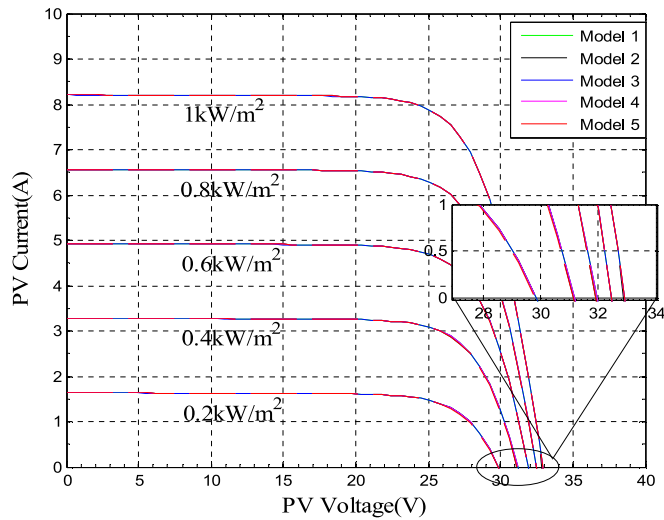
SHONGWE AND HANIF: COMPARATIVE ANALYSIS OF DIFFERENT SINGLE-DIODE PV MODELING METHODS

This article has been accepted for inclusion in a future issue of this journal. Content is final as presented, with the exception of pagination.

7

Fig. 6. *I–V* Characteristic for KC200GT module under varying irradiance for models 1, 2, 3, 4, and 5 using parameter estimation method B.
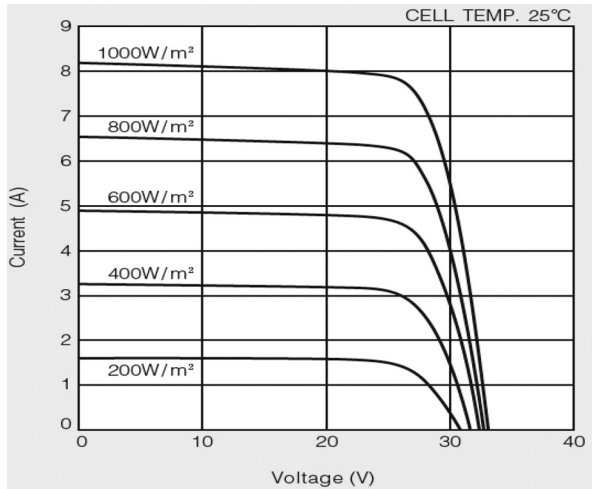

Fig. 7. *I–V* Characteristic for KC200GT module under varying irradiance extracted from datasheet.

Fig. 8. Experimental setup used to take measurements from SQ80 PV module.

Figs. 9 and 10 show *I–V* characteristic plots for the SQ80 simulated under varying temperature for all five models using method A and method B, respectively, and includes graphs plotted using measured data for the SQ80 module. It can be seen that using method A, the results obtained are more comparable with the measured values than for the one using method B, considering the shape of the curves toward the open-circuit
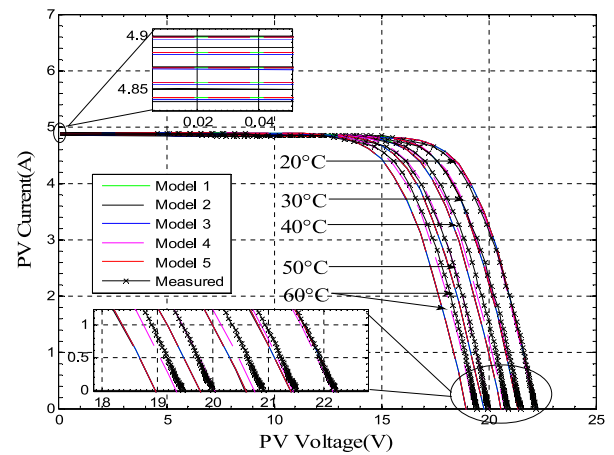

Fig. 9. *I–V* Characteristic for SQ80 module under varying temperature for models 1, 2, 3, 4, and 5 and measured values using parameter estimation method A.
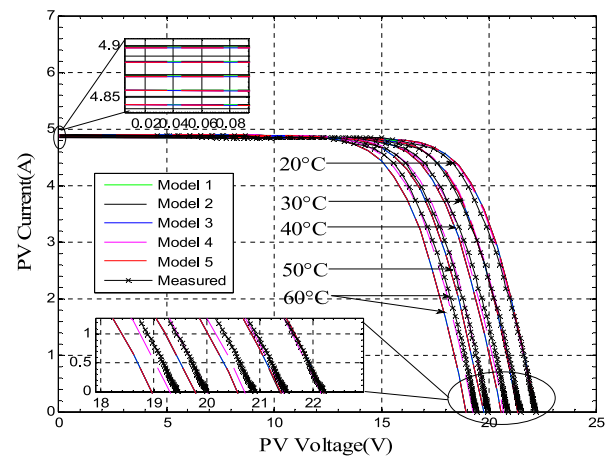

Fig. 10. *I–V* Characteristic for SQ80 module under varying temperature for models 1, 2, 3, 4, and 5 and measured values using parameter estimation method B.

voltage. The same effect can be seen from Figs. 11 and 12, which depict the plots from panel KC200GT using the two methods under varying temperature when compared with the datasheet extracted plots in Fig. 13.

The open-circuit voltage response to temperature variation from the different modeling methods as depicted in the plots show that at temperatures around the STC, the models depict similar behavior. However, as the temperature increases, one of the plots tends to deviate from the other corresponding plots i.e., model 4 deviates from models 1, 2, 3, and 5. It can be seen, however, that the graph that best approximates the plot using measured values with a small deviation is model 4.

Table V gives a summary of the variation of the open-circuit voltage and short-circuit current for the different models and estimation methods under varying temperature for the SQ80 module. The effect on the short-circuit current is the same for all methods, and this basically shows that there is minimal dependence between short-circuit current and changes in temperature. The effect of the difference in series resistance can be seen in the shape of the two graphs shown in Figs. 9 and 10
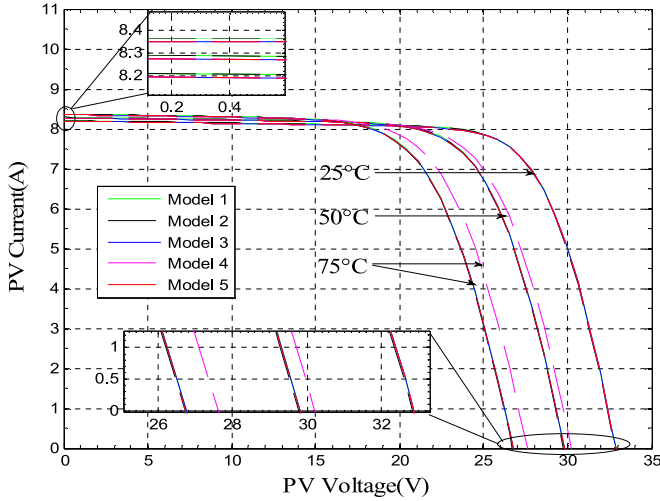
This article has been accepted for inclusion in a future issue of this journal. Content is final as presented, with the exception of pagination.

8   IEEE JOURNAL OF PHOTOVOLTAICS

Fig. 11.   *I–V* Characteristic for KC200GT module under varying temperature for models 1, 2, 3, 4, and 5 using parameter estimation method A.
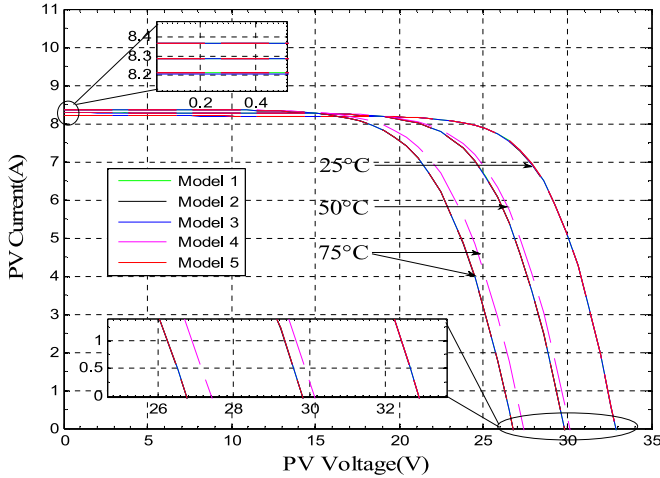

Fig. 12.   *I–V* Characteristic for KC200GT module under varying temperature for models 1, 2, 3, 4, and 5 using parameter estimation method B.
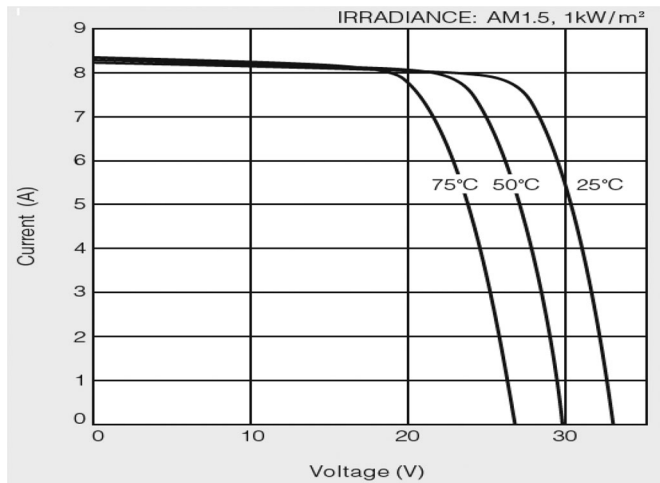

Fig. 13.   *I–V* Characteristic for KC200GT module under varying temperature extracted from datasheet.

TABLE V
SUMMARY OF GRAPHS UNDER VARYING TEMPERATURE

TEMP	Method A		Method B	
20 °C	Voc	Isc	Voc	Isc
Model 1	22.20484	4.843	22.20479	4.843
Model 2	22.20136	4.84300	22.20242	4.843001
Model 3	22.20451	4.84119	22.2046	4.842109
Model 4	22.15290	4.84300	22.15788	4.842109
Model 5	22.20484	4.84300	22.20461	4.842109
Measured	22.20	4.839	22.20	4.839
TEMP	Method A		Method B	
30 °C	Voc	Isc	Voc	Isc
Model 1	21.38991	4.85700	21.38825	4.857
Model 2	21.38632	4.85700	21.38576	4.856999
Model 3	21.38959	4.85518	21.38807	4.856106
Model 4	21.44186	4.85700	21.43454	4.856106
Model 5	21.38991	4.85700	21.38806	4.856106
Measured	21.50	4.851	21.50	4.851
TEMP	Method A		Method B	
40 °C	Voc	Isc	Voc	Isc
Model 1	20.58050	4.871	20.57906	4.871
Model 2	20.57704	4.870992	20.57669	4.870996
Model 3	20.58023	4.869179	20.57891	4.870103
Model 4	20.73592	4.870992	20.71694	4.870103
Model 5	20.58050	4.870992	20.57887	4.870103
Measured	20.90	4.872	20.90	4.872
TEMP	Method A		Method B	
50 °C	Voc	Isc	Voc	Isc
Model 1	19.77402	4.885	19.77372	4.885
Model 2	19.77043	4.884987	19.77121	4.884993
Model 3	19.77378	4.883173	19.77359	4.884101
Model 4	20.03502	4.884987	20.00486	4.884101
Model 5	19.77402	4.884987	19.77351	4.884101
Measured	20.00	4.890	20.00	4.890
TEMP	Method A		Method B	
60 °C	Voc	Isc	Voc	Isc
Model 1	18.95958	4.899	18.9579	4.898999
Model 2	18.95616	4.898982	18.95553	4.89899
Model 3	18.9594	4.897168	18.95782	4.898098
Model 4	19.33915	4.898982	19.29812	4.898098
Model 5	18.95958	4.898982	18.95769	4.898098
Measured	19.45	4.900	19.45	4.900

that the values produced from method A produces graphs which are more comparable with the plot with measured values.

IV. CONCLUSION

In this study, different modeling methods (equations) recommended by different authors in the literature are described (detailed under Section III) and have been verified by simulation and experimental results. The modeling equations that best approximate the plots from measured values for the SQ80 PV model, which is also applicable to any PV module with datasheet parameters, were recognized as shown by using a different module with different ratings from the SQ80 analyzed. Model 4 is justified in this case. The study also involved detailing the parameter estimation methods used within the five models that were classified. The parameter estimation has been identified to have an effect on the shape of the curve, as well as on the open-circuit voltage response under varying irradiance, as shown by the graphs. It can be concluded that the iterative method of extracting parameters, i.e., method A, produced more comparable results. Therefore, as long as there is convergence,

This article has been accepted for inclusion in a future issue of this journal. Content is final as presented, with the exception of pagination.

SHONGWE AND HANIF: COMPARATIVE ANALYSIS OF DIFFERENT SINGLE-DIODE PV MODELING METHODS
9

the iteration techniques produce more accurate results. This is mainly due to the fact that it includes all specific conditions of operation.

References

[1] P. Suskis and I. Galkin, "Enhanced photovoltaic panel model for MATLAB-simulink environment considering solar cell junction capacitance," in *Proc. IEEE 39th Annu. Conf. Ind. Electron. Soc.*, Nov. 10–13, 2013, pp. 1613–1618.

[2] S. Moodley. (2014, 13 Jun.). Renewables' contribution to SA's power mix set to grow. *Creamer Media's Eng. News.* [Online]. para. 1–9, Available: http://www.engineeringnews.co.za/article/renewables-to-contribute-42-to-national-energy-grid-by-2030-2014-06-13.

[3] F. Attivissimo, A. Di Nisio, M. Savino, and M. Spadavecchia, "Uncertainty analysis in photovoltaic cell parameter estimation," *IEEE Trans. Instrum. Meas.*, vol. 61, no. 5, pp. 1334–1342, May 2012.

[4] E. I. Batzelis, I. A. Routsolias, and S. A. Papathanassiou, "An Explicit PV string model based on the lambert function and simplified MPP expressions for operation under partial shading," *IEEE Trans. Sustainable Energy*, vol. 5, no. 1, pp. 301–312, Jan. 2014.

[5] F. Adamo, F. Attivissimo, A. Di Nisio, and M. Spadavecchia, "Characterization and testing of a tool for photovoltaic panel modeling," *IEEE Trans. Instrum. Meas.*, vol. 60, no. 5, pp. 1613–1622, May 2011.

[6] S. Gupta, H. Tiwari, M. Fozdar, and V. Chandna, "Development of a two diode model for photovoltaic modules suitable for use in simulation studies," in *Proc. Asia-Pacific Power Energy Eng. Conf.*, Mar. 27–29, 2012, pp. 1–4.

[7] S. Bal, A. Anurag, and B. C. Babu, "Comparative analysis of mathematical modeling of photo-voltaic (PV) array," in *Proc. IEEE Annu. India Conf.*, Dec. 7–9, 2012, pp. 269–274.

[8] M. Suthar, G. K. Singh, and R. P. Saini, "Comparison of mathematical models of photo-voltaic (PV) module and effect of various parameters on its performance," in *Proc. Int. Conf. Energy Efficient Technol. Sustainability*, Apr. 10–12, 2013, pp. 1354–1359.

[9] F. Spertino, J. Sumaili, H. Andrei, and G. Chicco, "PV module parameter characterization from the transient charge of an external capacitor," *IEEE J. Photovoltaics*, vol. 3, no. 4, pp. 1325–1333, Oct. 2013.

[10] M. Ahmad, A. A. Talukder, and M. A. Tanni, "Estimation of important parameters of photovoltaic modules from manufacturer's datasheet" in *Proc. Int. Conf. Inform., Electron. Vis.*, May 18–19, 2012, pp. 571–576.

[11] M. C. Di Piazza, M. Luna, and G. Vitale, "Dynamic PV model parameter identification by least-squares regression," *IEEE J. Photovoltaics*, vol. 3, no. 2, pp. 799–806, Apr. 2013.

[12] D. S. H. Chan and J. C. H. Phang, "Analytical methods for the extraction of solar-cell single- and double-diode model parameters from I-V characteristics," *IEEE Trans. Electron. Devices*, vol. ED-34, no. 2, pp. 286–293, Feb. 1987.

[13] S. Moballegh and J. Jiang, "Modeling, prediction, and experimental validations of power peaks of PV arrays under partial shading conditions," *IEEE Trans. Sustainable Energy*, vol. 5, no. 1, pp. 293–300, Jan. 2014.

[14] S. M. Petcut and T. Dragomir, "Solar cell parameter identification using generic algorithms," *J. Control Eng. Appl. Informat.*, vol. 12, no. 1, pp. 30–37, 2010.

[15] H. Andrei, T. Ivanovici, G. Predusca, E. Diaconu, and P. C. Andrei, "Curve fitting method for modeling and analysis of photovoltaic cells characteristics," in *Proc. IEEE Int. Conf. Autom. Quality Testing Robot.*, May 24–27, 2012, pp. 307–312.

[16] A. Chatterjee, A. Keyhani, and D. Kapoor, "Identification of photovoltaic source models," *IEEE Trans. Energy Convers.*, vol. 26, no. 3, pp. 883–889, Sep. 2011.

[17] Y. A. Mahmoud, X. Weidong, and H. H. Zeineldin, "A parameterization approach for enhancing PV model accuracy," *IEEE Trans. Ind. Electron.*, vol. 60, no. 12, pp. 5708–5716, Dec. 2013.

[18] S. A. Rahman, R. K. Varma, and T. Vanderheide, "Generalised model of a photovoltaic panel," *IET Renewable Power Gener.*, vol. 8, no. 3, pp. 217–229, Apr. 2014.

[19] S. J. Jun and L. Kay-Soon, "Optimizing photovoltaic model parameters for simulation," in *Proc. IEEE Int. Symp. Ind. Electron.*, May 28–31, 2012, pp. 1813–1818.

[20] H. A. B. Siddique, X. Ping, and R. W. De Doncker, "Parameter extraction algorithm for one-diode model of PV panels based on datasheet values," in *Proc. Int. Conf. Clean Electr. Power*, Jun. 11–13, 2013, pp. 7–13.

[21] Y. Mahmoud, W. Xiao, and H. H. Zeineldin, "A simple approach to modeling and simulation of photovoltaic modules," *IEEE Trans. Sustainable Energy*, vol. 3, no. 1, pp. 185–186, Jan. 2012.

[22] M. A. de Blas, J. L. Torres, E. Prieto, and A. Garcıa, "Selecting a suitable model for characterizing photovoltaic devices," *Renewable Energy*, vol. 25, no. 3, pp. 371–380, Mar. 2002.

[23] D. Sera, R. Teodorescu, and P. Rodriguez, "PV panel model based on datasheet values," in *Proc. IEEE Int. Symp. Ind. Electron.*, Jun. 4–7, 2007, pp. 2392–2396.

[24] S. J. Jun and L. Kay-Soon, "Photovoltaic model identification using particle swarm optimization with inverse barrier constraint," *IEEE Trans. Power Electron.*, vol. 27, no. 9, pp. 3975–3983, Sep. 2012.

[25] M. G. Villalva, J. R. Gazoli, and E. R. Filho, "Comprehensive approach to modeling and simulation of photovoltaic arrays," *IEEE Trans. Power Electron.*, vol. 24, no. 5, pp. 1198–1208, May 2009.

[26] H. Park and H. Kim, "PV cell modeling on single-diode equivalent circuit," in *Proc. IEEE 39th Annu. Conf. Ind. Electron. Soc.*, Nov. 10–13, 2013, pp. 1845–1849.

[27] M. M. H. Islam, S. Z. Djokic, J. Desmet, and B. Verhelst, "Measurement-based modelling and validation of PV systems," in *Proc. IEEE Grenoble PowerTech*, Jun. 16–20, 2013, pp. 1–6.

[28] L. Cristaldi, M. Faifer, M. Rossi, and F. Ponci, "A simple photovoltaic panel model: characterization procedure and evaluation of the role of environmental measurements," *IEEE Trans. Instrum. Meas.*, vol. 61, no. 10, pp. 2632–2641, Oct. 2012.

[29] H. Can, D. Ickilli, and K. S. Parlak, "A new numerical solution approach for the real-time modeling of photovoltaic panels," in *Proc. Asia-Pacific Power Energy Eng. Conf.*, Mar. 27–29, 2012, pp. 1–4.

[30] T. Salmi, A. Gastli, M. Bouzguenda, and A. Masmoudi, "MATLAB/Simulink based modelling of solar photovoltaic cell," *J. Renewable Energy Res.*, vol. 2, no. 2, 2012.

[31] M. A. Islam, A. Merabet, R. Beguenane, and H. Ibrahim, "Modeling solar photovoltaic cell and simulated performance analysis of a 250W PV module," in *Proc. IEEE Electr. Power Energy Conf.*, Aug. 21–23, 2013, pp. 1–6.

[32] Shell Solar, Photovoltaic solar module, SQ80 Datasheet.

[33] N. Femia, G. Petrone, G. Spagnuolo, and M. Vitelli, "PV modeling," in *Power Electronics and Control Techniques for Maximum Energy Harvesting in Photovoltaic Systems*. Boca Raton, FL, USA: CRC, 2013, pp. 11–15.

[34] Kyocera KC200GT datasheet. Available: http://www.kyocerasolar.com/assets/001/5195.pdf

Samkeliso Shongwe (M'14) was born in Manzini, Swaziland. He received the B.Eng. degree in electronic engineering from the University of Swaziland, Kwaluseni, Swaziland, in 2004, and is currently working toward the M.Sc. degree in electrical engineering with the University of Cape Town, Cape Town, South Africa.

His research interests include photovoltaic system modeling, maximum power point tracking of photovoltaic power, and grid integration of renewable energy sources.

Moin Hanif (M'11) received the first-class B.Eng.(Hons.) degree from the University of Nottingham, Nottingham, U.K., in electrical and electronic engineering in 2007 and the Ph.D. degree from the Dublin Institute of Technology, Dublin, Ireland, in November 2011.

He served both as a Part-time Assistant Lecturer with the Dublin Institute of Technology and as a Research Assistant with the Dublin Energy Lab-FOCAS Institute, from 2008 to 2011. He was a Postdoctoral Researcher with the Masdar Institute of Science and Technology, Abu Dhabi, UAE, from October 2011 to 2012. Since November 2012, he has been a Senior Lecturer with the Department of Electrical Engineering, University of Cape Town, Cape Town, South Africa. His research interests include the area of power electronics converters and their control, maximum power point tracking of photovoltaic power, islanding detection, grid integration of renewables, micro/smart grid operation, and wireless power transfer.

Dr. Hanif received a number of research grants from the University of Cape Town's Research Committee, Department of Science and Technology, National Research Foundation and ESKOM, South Africa. He received the Achievers Award scholarship from the University of Dublin. He serves as a Member on the Editorial Board of the *International Journal of Applied Control, Electrical and Electronics Engineering*, and also serves on a few Technical Program Committees for local and international conferences.